Improvement of carbon paper performance by adding carbon nanofibers to carbon paper and impregnation

J. Li, J. H. Dai, S.C. Zhang, C.H. Shen, J. Li[*], L.Z. Sha
School of Environmental and Natural Resources, Zhejiang University of Science & Technology, Hangzhou 310023, Zhejiang, China

Carbon paper, as a key component in proton exchange membrane fuel cells (PEMFCs), had attracted much attention due to its corrosion resistance, electrical conductivity and mechanical strength as well as gas permeability. The incorporation of carbon nanofibers (CNFs) into carbon paper can further enhance its electrical conductivity and other properties. Herein, prepared carbon paper precursors (CPP) via wet papermaking and optimized the process through resin impregnation and hot pressing. The addition of CNFs, particularly at 10 %, significantly improved electrical conductivity and mechanical properties, reducing resistivity by 23.9 % and maximizing tensile strength of 36.97 N·m/g. The sequence of CNFs application and resin impregnation, specifically the spray-after-impregnation (S-I) method, was crucial for achieving these enhancements. Our findings offer a strategy for fabricating high-performance carbon paper, crucial for PEMFC efficiency and durability.

1. Introduction

Proton exchange membrane fuel cells (PEMFC) have the advantages of low-temperature operation, fast start-up, high efficiency, and are a new type of environmentally friendly battery [1-5]. The gas diffusion layer of PEMFC plays important roles in conductivity, drainage, gas exchange, and supporting catalytic layer. The importance of gas exchange layer in PEMFC is self-evident. At present, carbon paper is often used as a gas diffusion layer in the PEMFC market [6]. Carbon paper is prepared by wet forming carbon fiber into carbon paper precursor (CPP), followed by resin impregnation, hot pressing, and heat treatment. However, the single C-C bond in carbon fiber is a non-polar covalent bond, which leads to a lack of active groups on the surface of carbon fiber, making it difficult to form carbon fiber and prepare CPP with high strength performance. The effect of resin impregnation is directly affected by the strength performance of CPP, which further affects the performance of the prepared carbon paper [7]. To give CPP a certain strength, the commonly used method is to add a binder, such as mixing polyvinyl alcohol (PVA) fibers with carbon fibers and using wet forming, drying and other processes to bond the carbon fibers to form CPP with a certain strength [8].

As a gas exchange layer for PEMFC, carbon paper requires excellent breathability, conductivity, and mechanical properties [9, 10]. The synergistic effect of commonly used reinforcing fibers such as plant fibers, regenerated cellulose fibers, and chemical fibers rich in active groups on the surface with binders can effectively improve the strength performance of CPP. Carbon fibers are mixed with other fibers, resulting in hydrogen bonds or other chemical bonds between the fibers [11]. Through wet papermaking, high-performance carbon paper can be prepared. By loading metal ions or heteroatoms on the surface of carbon fibers, the prepared carbon paper can have better conductivity as a gas exchange layer, improving the electrical performance of PEMFC [12-14].

Yang et al. [15] developed a two-step in-situ growth process to prepare carbon paper loaded with CeO_2/MnO_2 composite material (CeO_2/MnO_2-CFP) as an adhesive free photoelectrode for photo assisted electrochemical charge storage. Improved photoassisted charging capacity by approximately 20%. Jiang et al. [16] prepared and obtained cellulose carbon paper doped with iron, nickel, and sulfur as a catalyst for the cathodic reaction (ORR) of microbial fuel cells (MFCs) by adsorbing and recovering Congo red molecules from dye wastewater (Fe-N-S/CFs). Park et al. [17] prepared carbon paper by mixing cellulose fibers separated from yellow flowers with carbon fibers in a wet process. After carbonization at 1300 °C, the carbon paper exhibited the highest conductivity of 6.35 S cm^{-1}. Song et al. [18] synthesized graphite powders with different particle sizes (0.5-30 μm) Carbon paper is prepared by mixing with carbon fibers during wet manufacturing, containing 10 wt% polytetrafluoroethylene and graphite powder with a particle size of 30 μ. The electrochemical performance of carbon paper at m is the best, with a power density of 892 mW cm^{-2} and a maximum current density of 2.40 A cm^{-2}.

Carbon nanofibers (CNFs) are fibrous carbon materials with a micrographite crystal structure, which have superior mechanical properties, including high specific strength and high specific modulus, as well as low density, low thermal expansion, heat resistance, chemical stability, and other characteristics [19-21]. They are currently widely used in the food industry, aerospace, medical equipment, environmental protection, supercapacitors and other fields. Zhao et al.[22] prepared nanocomposites using carbon nanofiber paper and concluded that the properties of carbon paper are closely related to the manufacturing conditions. At present, CNFs filling technology is still in a vacuum zone with development in the production of carbon paper. However, the excellent performance of CNFs combined with adhesive fibers is very suitable for the interweaving of carbon fibers in carbon paper. This paper aims to use spray gun to spray CNFs onto carbon paper after hot pressing, which is prepared by wet papermaking, and cooperate with phenolic resin impregnation step, so as to enhance the physical and mechanical properties and electrical conductivity of carbon paper.

2. Experiment

2.1. Materials

4mm carbon fiber (Toei Corporation, Japan); Carbon nanofibers (Beijing Deke Island Gold Co., Ltd.); Polyvinyl alcohol fiber (Shanghai Chenqi Chemical Technology Co., Ltd.); Polyethylene oxide (McLean).

2.2. Experimental instruments

Paper forming machine (TD10-200, Xianyang Tongda Light Industry Equipment Co., Ltd.); Single layer electric flat vulcanization machine (XB-30T, Zhejiang Tiandu Technology Co., Ltd.); Thermogravimetric analyzer (SDT 650, TAInstruments, USA); Double arm microcomputer tensile tester (KYD-2000NS, Zhejiang Tiandu Technology Co., Ltd.); Breathability tester (FX 3300, Textest, Switzerland); Four probe tester (RTS-8, Guangzhou Four Probe Technology Co., Ltd.); Thickness measuring instrument (PT-4, Hangzhou Qingtong Boke); Horizontal stiffness tester (WTD-1000, Hangzhou Qingtong Boke); Scanning electron microscopy (S3400, Shimadzu, Japan); Fiber dissociator (T015-A, Xianyang Tongda Light Industry Equipment Co., Ltd.)

2.2. Experimental methods

2.2.1. Papermaking

Add 1.4 g of carbon fiber and 0.4 g of PVA fiber to a polyethylene oxide (PEO) aqueous solution for dispersion, and stir with a stirrer to evenly disperse the carbon fiber. Using the wet papermaking process, a paper forming machine is used to produce 60 ± 3 g/m2 carbon paper, which is then dried to obtain the carbon paper raw material.

2.2.2. Impregnated resin, cured and formed

Prepare a phenolic resin ethanol solution (volume ratio 11:89) as an impregnating agent. Take an appropriate amount of impregnating agent and immerse the carbon paper raw material in it for a period of time. Take it out and dry it, and press it on a flat vulcanizing machine at 140°C for 20 minutes.

2.2.3. CNFs filling

Add CNFs to a 20 ml ethanol solution for dispersion, and stir with a stirrer to evenly disperse the carbon fibers. Before or after impregnating the resin, use the spray gun to add CNFs spray to the surface of carbon paper.

2.3. Detection and characterization

2.3.1. Thickness

The thickness of carbon paper can affect its performance, and being too thin or too thick can have adverse effects on the performance of the battery. The thickness of carbon paper is measured using a thickness gauge model from Hangzhou Qingtong Boke's thin film thickness tester (PT-4). Using the mechanical contact method, select a 5 * 5cm paper sample with at least 9 testing points, and calculate the average thickness d of the carbon paper sample.

2.3.2. Air Permeability

Analyze the air permeability of carbon paper base paper using breathability tester (FX 3300, Textest, Switzerland). Place the original paper on the stage of the permeability tester, select a testing area of 20 cm^2, and a testing pressure of 400 Pa. Analyze according to the instrument's usage method. After the instrument reading remains stable, record the data. Each sample should be tested for air permeability at least 5 times, and the average value should be taken to determine the air permeability of the sample.

2.3.3. Electrical resistivity

Use the Four probe tester (RTS-8, Guangzhou Four Probe Technology Co., Ltd.) to measure the electrical resistivity of carbon paper base paper. Firstly, estimate the resistivity range of the sample based on its size and select the corresponding range. Place the sample, press down on the probe, and connect the current to the sample. Calculate the required test resistivity based on the size of the sample and instrument parameters, and adjust the potentiometer to display the required test current on the host. Then adjust the mode so that the host displays the test results. At least 9 points should be tested on each sample, and the average value should be measured to determine the electrical resistivity of the sample.

2.3.4. Tensile strength

Measure the tensile strength of carbon paper base paper using double arm microcomputer tensile tester (KYD-2000NS, Zhejiang Tiandu Technology Co., Ltd.). Cut the sample into a paper strip with a width of 15 mm, use the fixture of the instrument to clamp both sides and gradually apply tension until the paper sample breaks, and obtain its tensile strength. Each group of samples shall be tested for tensile strength at least nine times, and the average value shall be calculated to obtain the tensile strength of the samples.

2.3.5. Microscopic morphology

A scanning electron microscope (SEM, S3400, Shimadzu, Japan) was used to capture the microstructure of the copy paper, the sample was cut into small pieces of paper, sprayed with gold and photographed.

3. Results and discussion

3.1. Detection of CNFs

Fig. 1(a) showed the SEM image of CNFs prepared by chemical deposition method, with relatively smooth and rod-like surface, spherical fiber head, irregular distribution of fiber arrangement, diameter in the range of 50-150 nm, and length in the micrometer range. Fig. 1(b) showed the SEM image of CNFs prepared by electrostatic spinning, which showed more serious clustering phenomenon. Fig. 1(c) showed the elemental analysis results of CNFs prepared by chemical deposition method, whose main constituent elements are C, accounting for 99.64%, and O, accounting for 0.36%. The CNFs have high content of C elements and fewer heterogeneous elements, which were more suitable to be used for the filling of carbon paper in the proton exchange membrane of fuel cells. Fig. 1(d) showed the elemental analysis results of CNFs prepared by electrostatic spinning method, the C content is 98.71%, and there are more impurity elements, so it was not selected as the raw material of CNFs for the subsequent experiments.
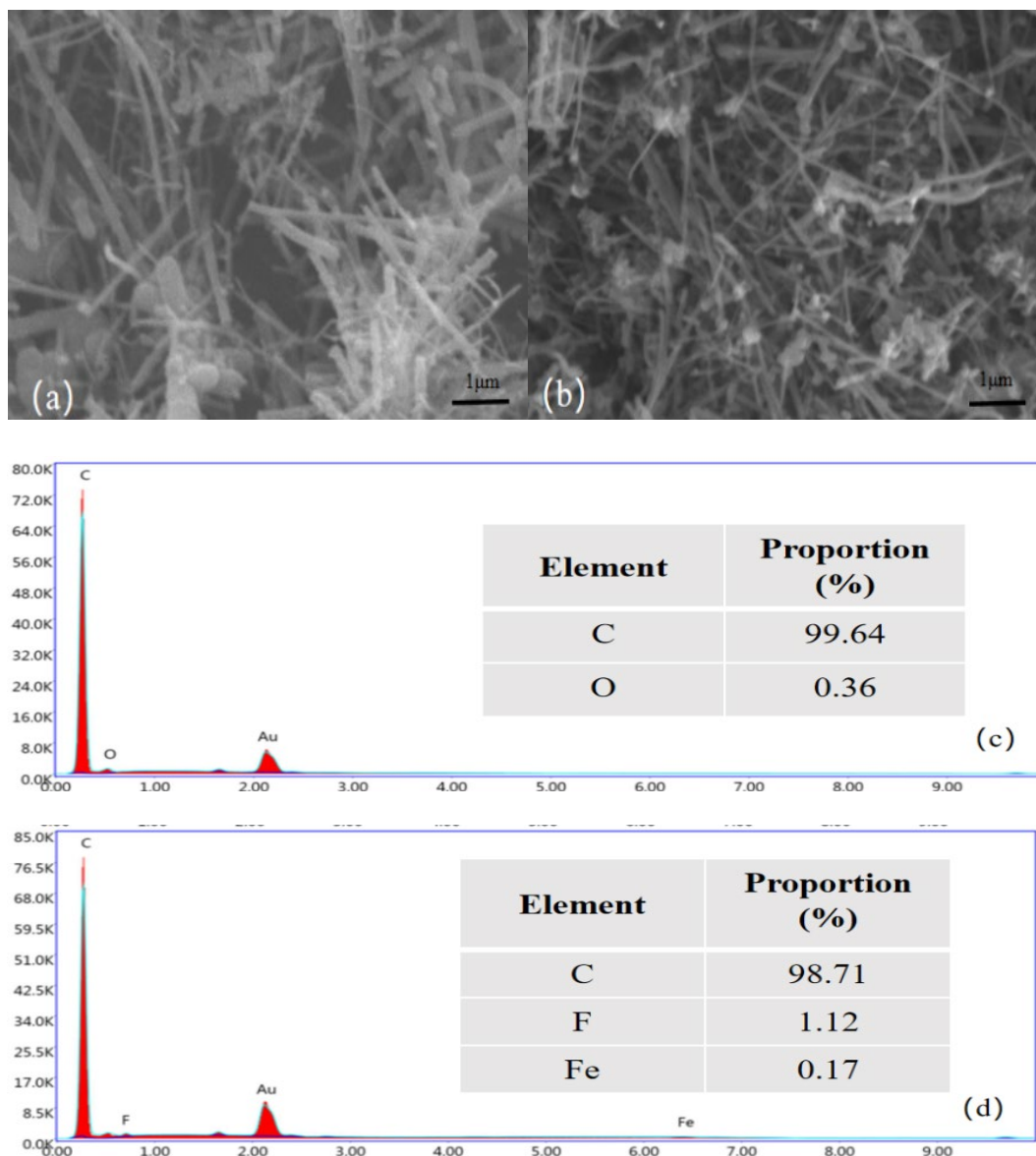
Fig. 1. Analysis of CNFs (a)Microscopic morphology of CNFs (b) element analysis report of CNFs.

3.2. Detection of CNFs coated carbon paper

3.2.1. Analysis of carbon paper

Fig. 2 showed the carbon paper with different amounts of CNFs added. The surfaces of C-1%, C-5% and C-10% carbon paper in Fig. 2(b-d) were dense and uniform, and the C-10% carbon paper has a slight flexibility and can be bent at a small angle, and the surface is smoother and the paper flexibility was improved compared with that of the C-0% control group in Fig. 2(a). The rough surface of the C-15% and C-20% carbon paper in Figure 2(e,f) may be caused by the uneven dispersion due to the excessive addition of CNFs. From the results of C-10% elemental analysis in Fig. 2(g), it could be seen that the main constituent element of carbon paper is C, which accounted for 97.65%. 3% of O, 0.4% of Al and 0.85% of Si. Carbon fibers with high C elemental content have better electrical conductivity.
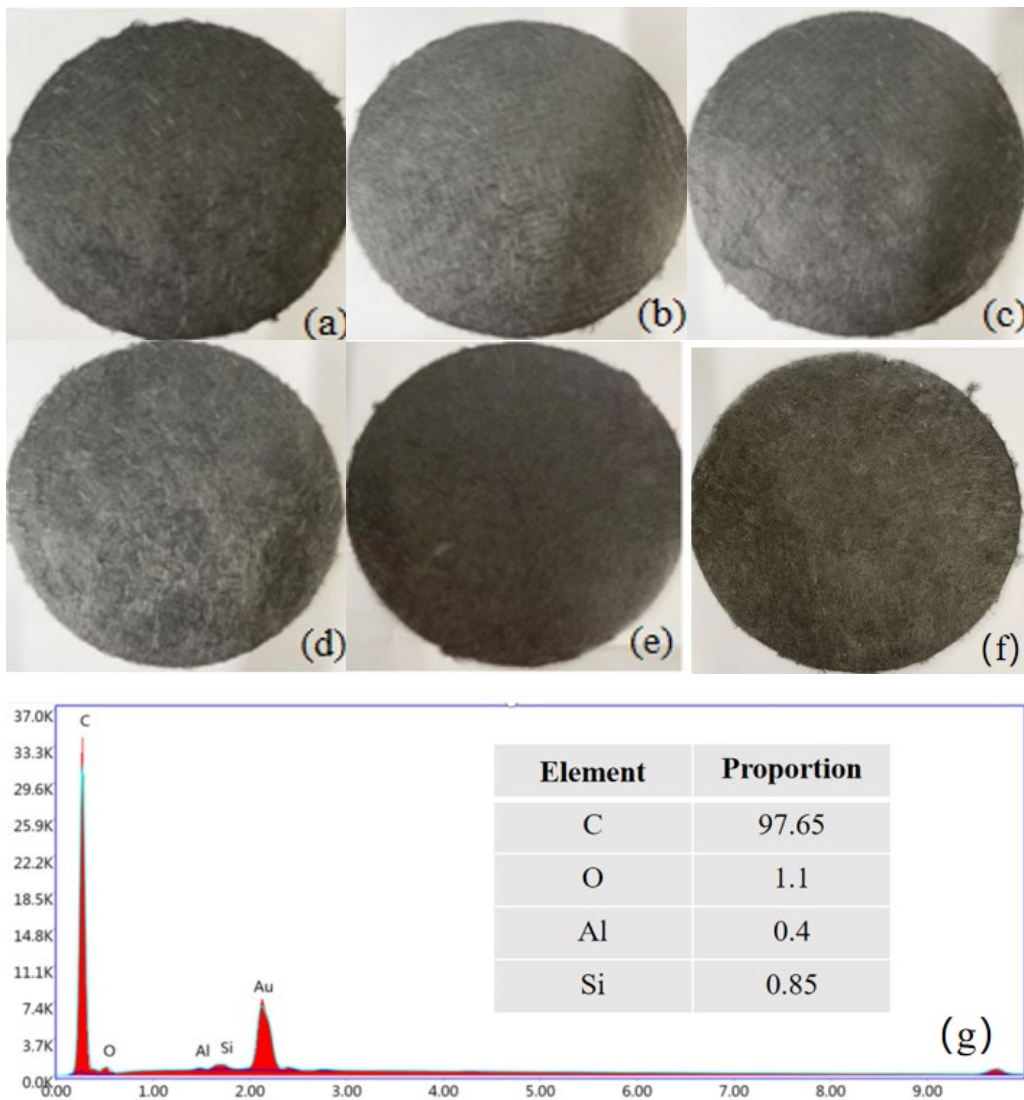
Fig. 2. Carbon paper physical appearance (a) 1% (b) 5% (c) 10% (d) 15% (e) 20%
(f) 0%and(g) element analysis.

3.2.2. Microscopic morphology of carbon paper

Fig. 3 showed the SEM images of carbon paper with different amounts of CNFs added. As shown in the figure, irregular interweaving is formed between the carbon fibers, and PVA fibers are filled into the inter-fibers to produce a lap bridge connection. Fig. 3(a,b) showed the SEM images of C-1% and C-5% carbon paper, from which it could be seen that there were a small number of PVA fibers connecting between the carbon fibers. Fig. 3(c) showed the SEM image of C-10% carbon paper, in which a large number of PVA fibers are adhered between carbon fibers and CNFs were randomly attached to PVA fibers and carbon fibers. Fig. 3(d,f) showed the SEM images of C-15% and C-20% carbon paper, in which it can be found that with the increase of CNFs addition, there were more CNFs adhered to PVA fibers after hot-melting, although the over-adhesion may make the surface of the paper sheet rough, but it may improve the mechanical properties of carbon paper due to the improvement of the connectivity density between the carbon fibers.
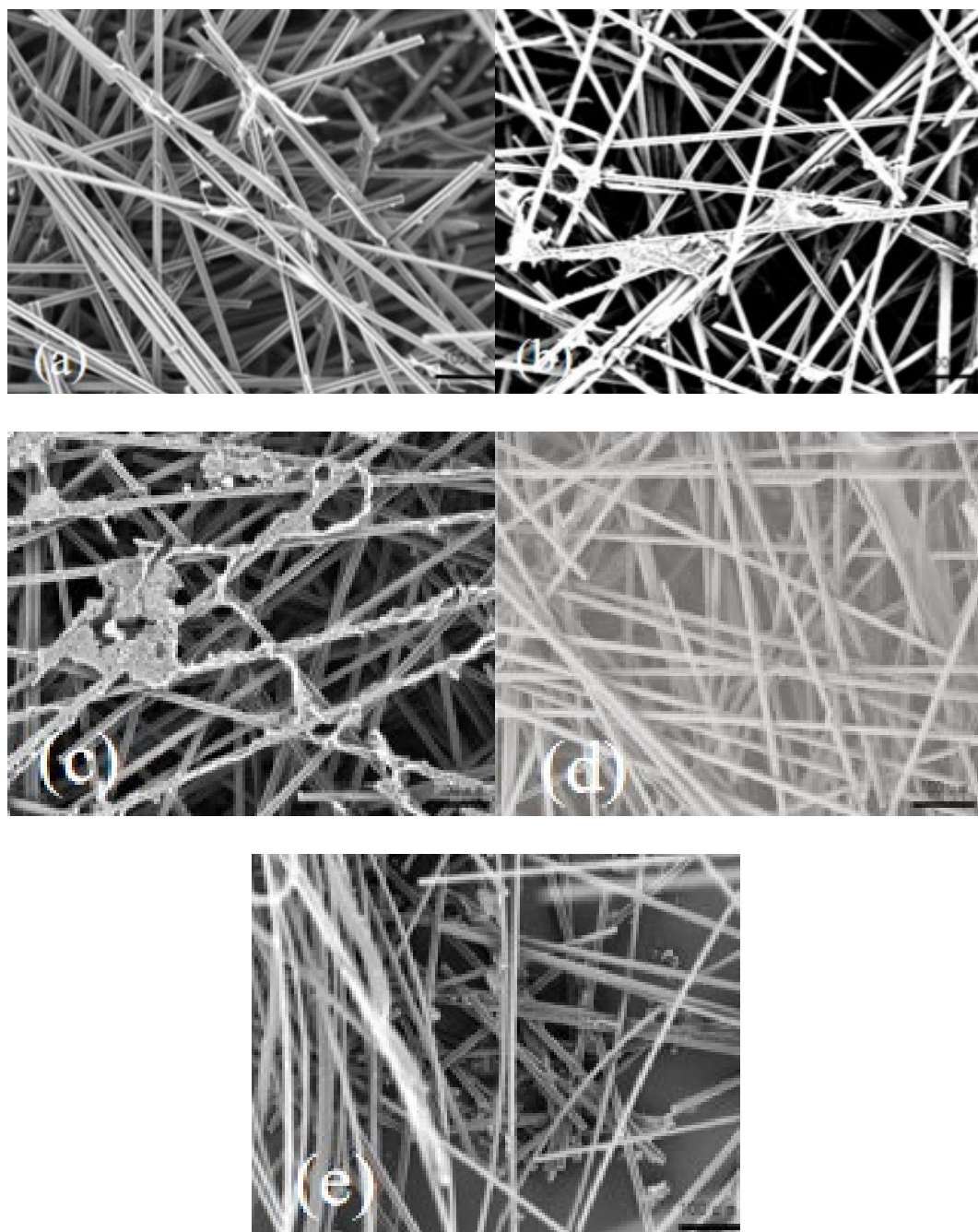
Fig. 3. Microscopic morphology of carbon paper with different amount of CNFs added (a) C-1% (b) C-5% (c) C-10% (d) C-15% (e) C-20%.

3.2.3. The breathability of carbon paper

Fig. 4 showed the relevant test graphs about the permeability of carbon paper. Fig. 4(a) showed the air permeability graph of carbon paper, as shown in the figure the air permeability of carbon paper without CNFs addition was 1350 mm/s, which had good air permeability performance. With the increase of CNFs addition, the permeability of carbon paper showed a decreasing trend. When the amount of CNFs added is 10%, the permeability was 1100 mm/s, and when the amount

of CNFs added is 15%, the permeability is 1010 mm/s. Fig. 4(b) showed the porosity graph of carbon paper, from which it can be seen that as the amount of CNFs added increases, the porosity curve of the carbon paper decreases gradually, and the porosity of CNFs added is 89% when the amount of CNFs added was 1%, 86% when the amount of CNFs added is 10%. The porosity curve of carbon paper decreases gradually with the increase of CNFs addition, the porosity is 89% at 1% CNFs addition, 86% at 10% CNFs addition, and 84% at 15% CNFs addition, and the effect of the increase of CNFs addition on the porosity showed a gradual decreasing trend.
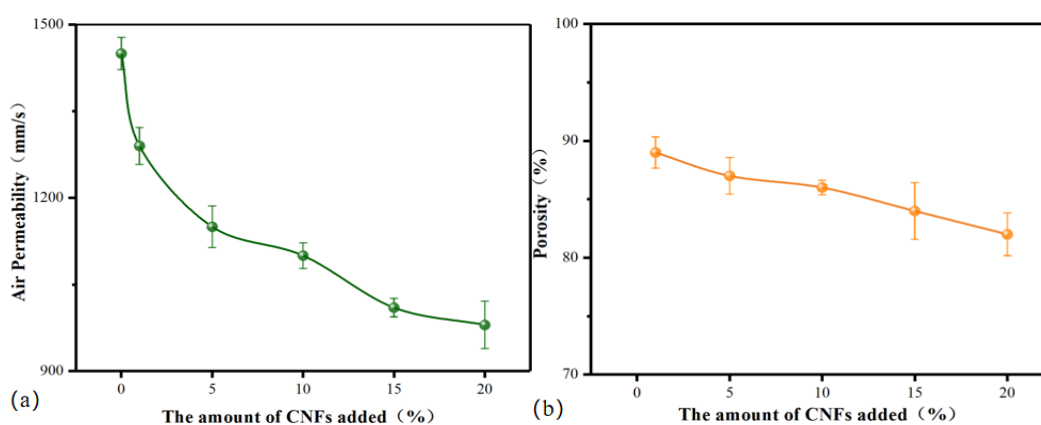
Fig. 4. Effects of adding different amounts of CNFs on carbon paper (a) air permeability (b) porosity pattern.

3.2.4. Resistivity of carbon paper

Fig. 5 shows the resistivity curves of carbon paper with different amounts of CNFs added. From the figure, it could be seen that the resistivity of carbon paper decreases with the addition of CNFs. the C-10% sample has the lowest resistivity of 17.98 mΩ·cm, which was 23.9% lower compared to the C-0% sample, which had the best conductivity. This may be due to the fact that the addition of CNFs improved the structural voids between the carbon fibers in the carbon paper, which increased the conductive pathway. When the CNFs filling amount was increased to 15-20%, the resistivity does not decrease further, which was possibly because the excess CNFs are trapped by the surface of the carbon paper and do not penetrate deeply into the internal pores of the carbon paper. Therefore, in terms of the resistivity trend, 10% CNFs addition is optimal.
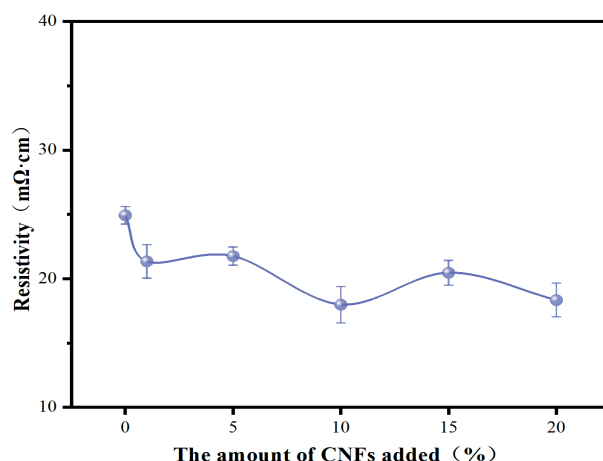
Fig. 5. Effect of adding different amounts of CNFs on carbon paper resistivity.

3.2.5. Mechanical properties of carbon paper

Fig. 6 showed the mechanical properties associated with carbon paper with different amounts of CNFs added. From Fig. 6(a), it could be seen that the stiffness of C-0% paper is 0.32 mN·m, and with the increase of the filling amount, the stiffness increased and then decreases. When the filling amount reaches 5%, the stiffness of carbon paper reaches the maximum value of 4.28 mN·m, and when the filling amount reaches 20%, the stiffness is 0.83 mN·m, which may be due to the increase in the filling amount of CNFs, resulting in the brittleness of the carbon paper, which affected the stiffness of carbon paper. From Fig. 6(b), it can be seen that the tensile strength increases and then decreases with the increase of CNFs filling amount. The tensile strength of carbon paper with 10% CNFs was 36.97 N·m/g, which is the best among the carbon paper samples filled with CNFs. When the filling amount of CNFs exceeds 10%, the tensile strength decreased with the increase of filling amount. The worst improvement was observed at 20% filling level, with a tensile strength of 7.88 N·m/g, which is still a small improvement compared with the carbon paper.
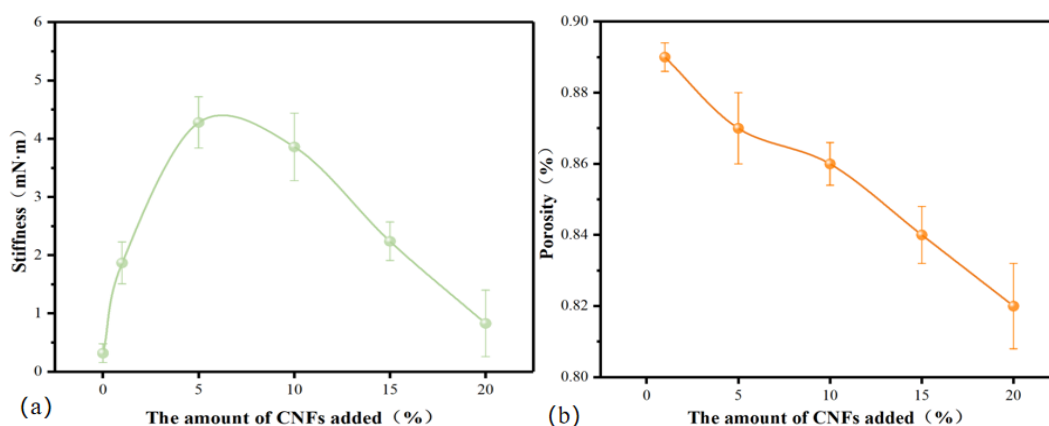
Fig. 6. Effect of adding different amounts of CNFs on (a) stiffness (b) tensile strength.

3.2.6. Thermal stability of carbon paper

Fig. 7 showed the thermogravimetric diagrams of carbon paper with different amounts of CNFs under the conditions of incineration temperature of 800℃ and nitrogen as the atmosphere. From the figure, it could be seen that when the filling amount of CNFs is less than 10%, with the increase of filling amount, the residual mass shows a rising trend, and the residual mass of C-10% carbon paper was as high as 81.74%, and after the filling amount of CNFs was more than 10%, the folding line shows a decreasing trend, especially the residual mass of C-20% carbon paper is only 77.05%. When the CNFs were overfilled, agglomeration occurs and was deposited on the surface of the carbon paper, which affected the thermal stability of the carbon paper.
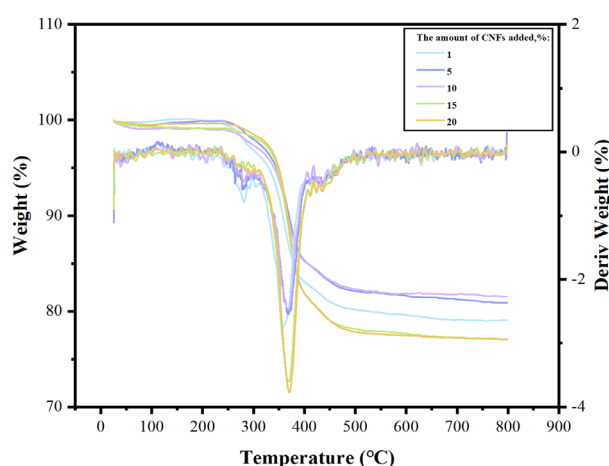
Fig. 7. Effect of adding different amounts of CNFs on the thermal stability of carbon paper.

3.3. The influence of process sequence on the performance of carbon paper

In the traditional manufacturing process of carbon paper, the mechanical properties of carbon paper are enhanced by impregnation with phenolic resin. Therefore, this experiment added a modification step for impregnating carbon paper with phenolic resin. The modification of the copied carbon paper base paper involves two steps: spraying CNFs and impregnating, and the process of spraying CNFs first and then impregnating the carbon paper into phenolic resin is recorded as S-I; The process of impregnation followed by spraying is referred to as I-S; The process of dispersing CNFs into phenolic resin and then impregnating them is referred to as S&I.

3.3.1. Physical image and microscopic morphology of carbon paper

Fig. 8 showed the physical images and microscopic morphology of the carbon paper obtained after S-I, I-S and S&I preparation processes at 140℃, 2.0 MPa, and hot pressing for 20 min. The surface of the carbon paper was smooth, and there are CNFs attached on the surface of the carbon paper by the three preparation processes. Among them, a large number of CNFs were attached on the surface of carbon paper treated by the I-S process. On the other hand, there were fewer CNFs on the surface of the carbon paper treated by S-I and S&I, and the post-impregnation hot-pressing step might have brought most of the CNFs into the carbon paper. At the microscopic level, the carbon fibers had smooth surfaces and were interlaced, and the fibers were bonded by hot-

melted PVA fibers. Under the three process conditions, CNFs were attached to the surface of the carbon paper and between fibers inside it, and the amount of attachment increased with the addition amount. After the S-I process, more CNFs were uniformly attached to the fibers inside the carbon paper, and the bridging effect of CNFs made the fibers inside the carbon paper tightly connected, with small inter-fiber gaps. However, the flocculation of CNFs increased with the increase of CNFs addition. The surface of carbon paper treated by I-S process retains most of the CNFs, and the connection between fibers inside the carbon paper was insufficient, and the flocculation situation was more serious. CNFs are distributed on the surface and inside of S&I carbon paper, and the spraying and impregnation steps were carried out at the same time, and when the phenolic resin was impregnated into the inside of the carbon paper, it will bring the CNFs into the carbon fibers and PVA fibers, and then it will be connected with the bridging effect between the fibers after the hot compression molding, but the CNFs do not reach 100% retention. The CNFs did not reach 100% retention.
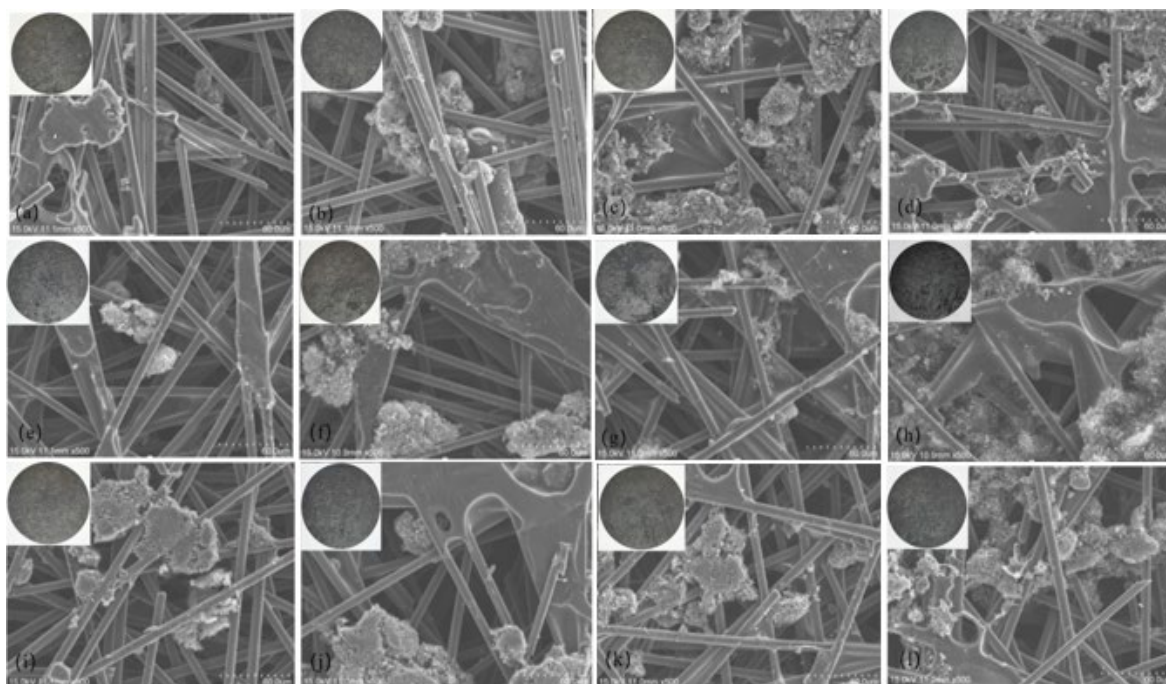
Fig. 8. Carbon paper prepared at 140℃ and 2.0 MPa hot pressing condition (a) S-I-5% (b) S-I-10% (c) S-I-15% (d) S-I-20% (e) I-S-5% (f) I-S-10% (g) I-S-15% (h) I-S-20% (i) S&I-5% (j) S&I-10% (k) S&I-15% (l) S&I-20% Physical image and microscopic morphology.
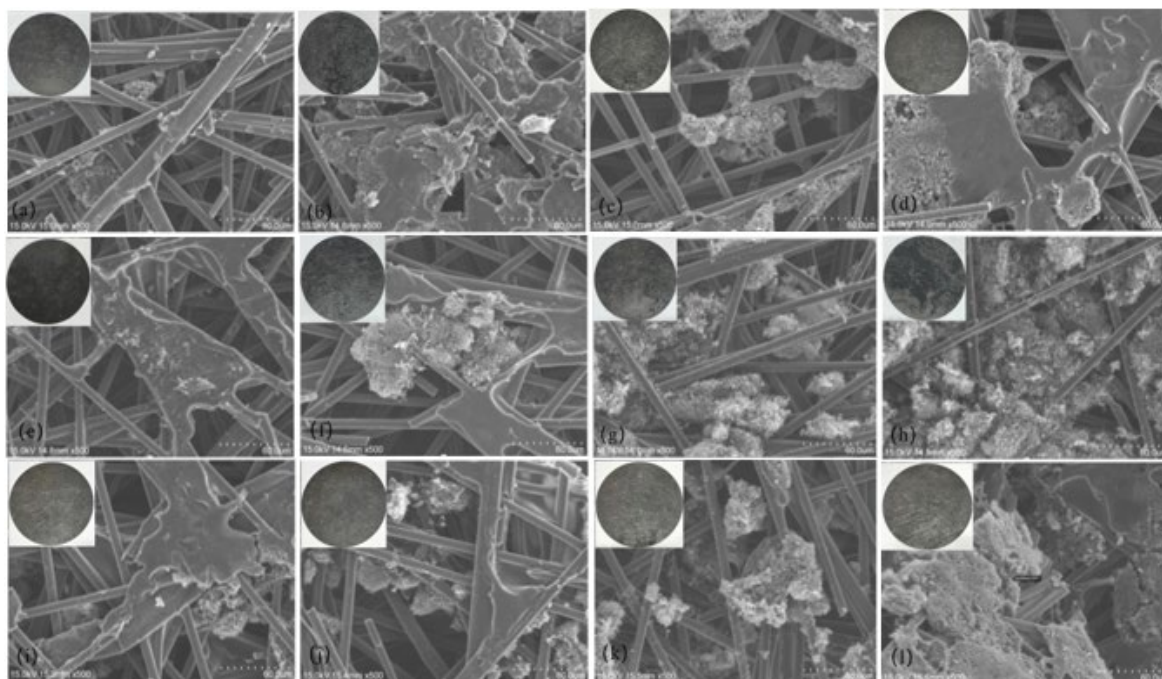
Fig. 9. Carbon paper prepared at 140℃ and 2.5 MPa hot pressing condition (a) S-I-5% (b) S-I-10% (c) S-I-15% (d) S-I-20% (e) I-S-5% (f) I-S-10% (g) I-S-15% (h) I-S-20% (i) S&I-5% (j) S&I-10% (k) S&I-15% (l) S&I-20% Physical image and microscopic morphology.

Fig. 9 showed the physical image and microscopic morphology of the carbon paper obtained after the S-I, I-S and S&I preparation process at 140℃, 2.5 MPa, and hot pressing for 20 min. From the figure, it could be seen that the surface of carbon paper has some CNFs attached, and the paper was flexible and not easy to break. From the SEM image, it could be found that with the increase of the addition of CNFs, the attachment of CNFs on the surface of carbon paper and its interior increases. From Figure 9 (a-d), it could be found that a large number of CNFs are obviously visible between the fibers inside the S-I carbon paper, and the post-impregnation step effectively brings the CNFs onto the hot-melted PVA fibers inside the carbon paper, attaching them and making the connection between the fibers tight. The flocculation situation of the CNFs was aggravated with the increased in the amount of CNFs added. From Fig. 9 (e-h), it could be seen that most of the CNFs were attached to the surface of I-S carbon paper, and the inter-fiber connection was less, so it lead to a larger and uneven pore space inside the carbon paper, and there was less effective connection between the carbon paper fibers. It could be observed that the flocculation phenomenon on the surface of I-S-20% carbon paper with high CNFs filling was very serious. In Fig. 9 (i-l), it could be observed that CNFs exist uniformly on the surface and inside of the S&I carbon paper, but the amount is obviously less than the other two processes, which was due to the loss of part of the CNFs in the impregnating solution, and the pores inside the carbon paper are smaller.
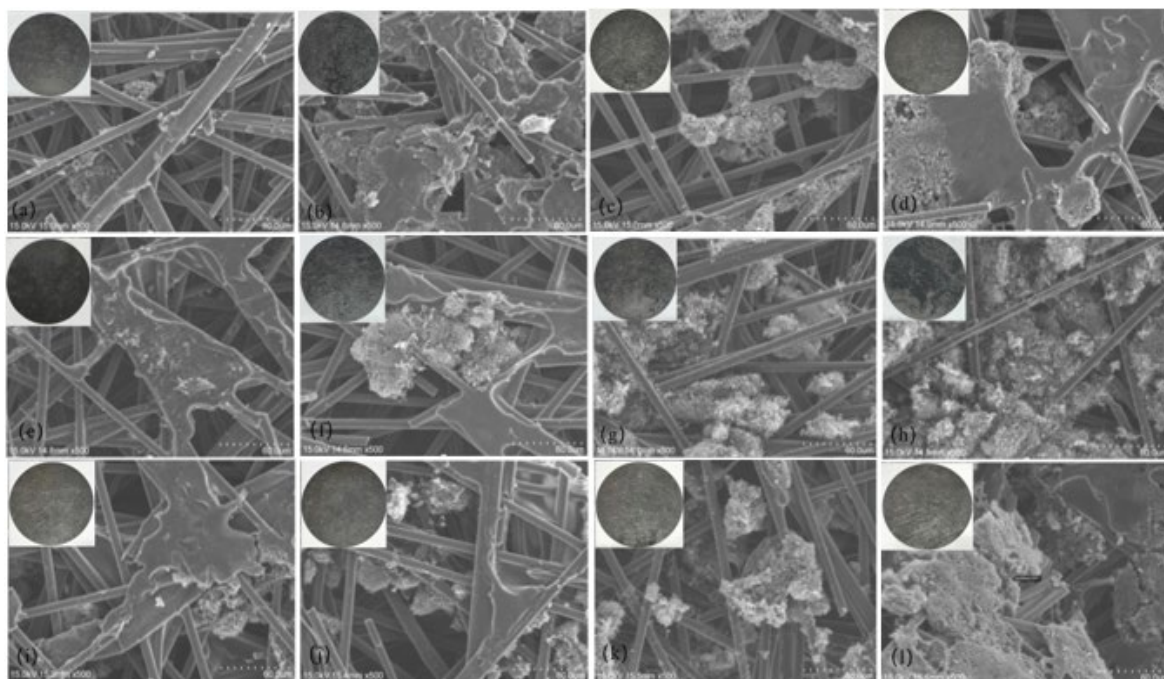
Fig. 10. Carbon paper prepared at 140°C and 3.0 MPa hot pressing condition (a) S-I-5% (b) S-I-10% (c) S-I-15% (d) S-I-20% (e) I-S-5% (f) I-S-10% (g) I-S-15% (h) I-S-20% (i) S&I-5% (j) S&I-10% (k) S&I-15% (l) S&I-20% Physical image and microscopic morphology.

Fig. 10 showed the physical image and microscopic morphology of the carbon paper obtained by the S-I, I-S and S&I preparation process under the hot pressing conditions of 140°C, 3.0 MPa and 20 min. From the figure, it could be seen that the carbon paper surface is smooth, the fibers are uniformly interlaced, with a certain degree of flexibility, can be folded at a small angle, and there are CNFs attached to the surface. Fig. 10 (a-d) showed that there are hot-melted PVA fibers connecting the carbon fibers inside the S-I carbon paper, and the CNFs are attached to them, forming a close bridge structure. Fig. 10 (e-h) showed the carbon paper after I-S process, the PVA fibers remain on the surface after hot melting, most of the CNFs are attached to them, the pores between the fibers are large, and the flocculation of CNFs on the surface is serious. Fig. 10 (i-l) showed the physical image and microscopic morphology of S&I carbon paper, from which it could be found that there are some CNFs on the surface of the carbon paper and the interior of the carbon paper. CNFs with the phenolic resin immersed into the carbon paper interior, the CNFs along with the attachment of the carbon fibers and PVA fibers on top of the carbon fibers, but the amount of CNFs because of the retention rate of less than 100%, significantly less than the other two processes of the carbon paper. The pores inside the carbon paper are small.
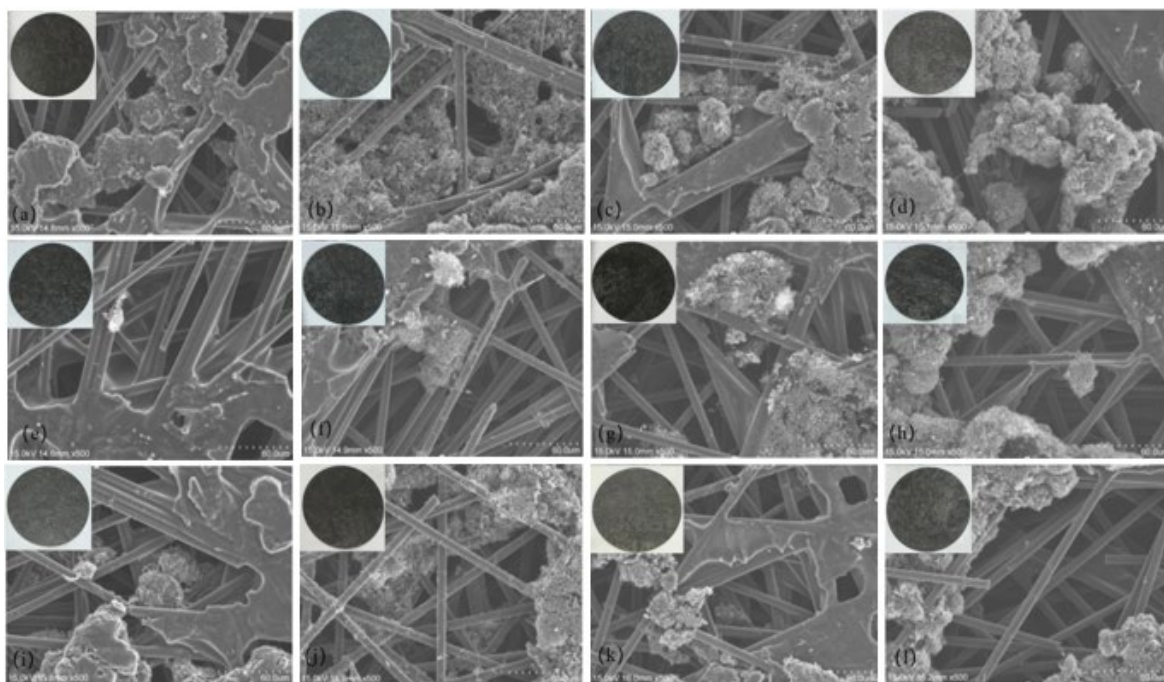
Fig. 11. Carbon paper prepared at 150℃ and 2.0 MPa hot pressing condition (a) S-I-5% (b) S-I-10% (c) S-I-15% (d) S-I-20% (e) I-S-5% (f) I-S-10% (g) I-S-15% (h) I-S-20% (i) S&I-5% (j) S&I-10% (k) S&I-15% (l) S&I-20% Physical image and microscopic morphology.

Fig. 11 showed the physical as well as SEM images of the carbon paper obtained by the S-I, I-S, and S&I preparation processes at 150℃, 2.0 MPa, and hot pressing for 20 min. From the figure, it could be found that the internal fibers of the carbon paper are uniformly distributed, and with the increase of the addition of CNFs, the attachment of CNFs on the surface of the carbon paper as well as on the internal fibers increases. The carbon paper paper samples have some flexibility and could be slightly bent and not easily broken. Observation of Fig. 11 (a-d) showed that a large number of CNFs exist in the internal fibers of the S-I carbon paper, and only a small portion of CNFs remain on the surface of the carbon paper, which may be due to the fact that CNFs enter the pores of the carbon paper with the impregnating solution and remain on the hot-melt PVA fibers inside the carbon paper after hot press molding. The attachment of these CNFs made the connection between the carbon paper fibers tighter and the pores smaller compared with the other two preparation processes. From Fig. 11 (e-h), it could be seen that most of the CNFs are attached to the surface of I-S carbon paper, and a very small amount of CNFs enters into the interior of the carbon paper to fill the voids. With the increase of CNFs addition, the flocculation situation is aggravated. The pores inside the carbon paper were large and uneven. In Fig. 11 (i-l), it could be found that some CNFs exist on the surface and inside of the S&I carbon paper, but some of the CNFs remain in the impregnating solution during the impregnation step, and the coating is not 100%, resulting in the amount of CNFs inside the carbon paper was significantly less than the other two processes, and the pores were smaller and more uniform than those in the I-S carbon paper samples.
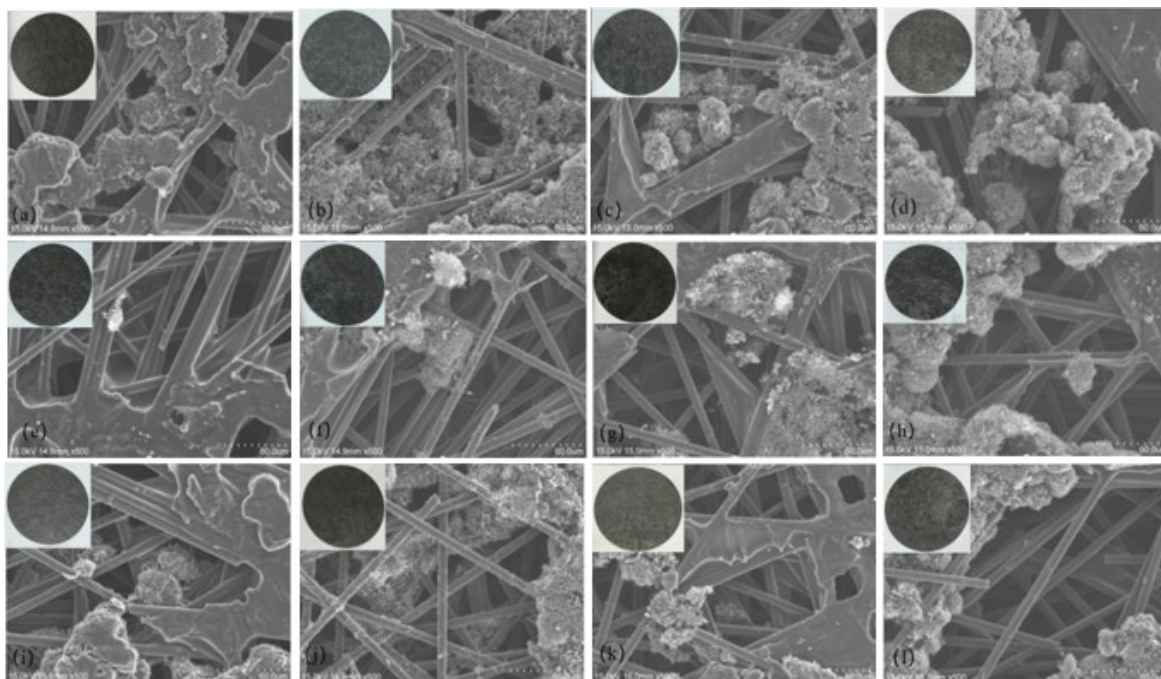
Fig. 12. Carbon paper prepared at 150°C and 2.5 MPa hot pressing condition (a) S-I-5% (b) S-I-10% (c) S-I-15% (d) S-I-20% (e) I-S-5% (f) I-S-10% (g) I-S-15% (h) I-S-20% (i) S&I-5% (j) S&I-10% (k) S&I-15% (l) S&I-20% Physical image and microscopic morphology.

Fig. 12 showed the physical images and microscopic morphology of the carbon paper obtained by the S-I, I-S, and S&I preparation processes and hot pressing at 150°C, 2.5 MPa, and 20 min. From the figure, it could be seen that there were some CNFs attached on the surface of each carbon paper, and the amount of CNFs inside the carbon paper was linked to the filling process. The carbon paper was thin, flexible and tough, and can be slightly bent and not easily broken. From the microscopic morphology, it could be seen that the fibers inside the carbon paper are interlaced, the hot-melted PVA fibers were connected to the carbon fibers, and the CNFs were uniformly distributed on them after spray coating. From Fig. 12 (a-d), it can be found that CNFs are uniformly attached to the internal fibers of S-I carbon paper, and their synergistic effect with the hot-melted PVA fibers made the carbon paper fibers connect tightly and fills up the voids between the fibers inside the carbon paper. Therefore, the internal gap of S-I carbon paper was the smallest among the three preparation processes. From Fig. 12 (e-h), it could be found that CNFs are more retained on the surface of I-S carbon paper, resulting in insufficient effective connection between the fibers inside the carbon paper, and the void is larger, which affected a series of properties of the carbon paper. With the increase of CNFs addition, the flocculation phenomenon is aggravated. Fig. 12 (i-l) showed the physical image and microscopic morphology of S&I carbon paper, from the figure it could be found that the amount of CNFs effectively attached to the carbon paper of this process was significantly less than the other two processes, the reason for this was that the CNFs are not 100% sprayed, and a part of the CNFs remain in the impregnating solution, so the pores are larger than those of the S-I carbon paper, and the CNFs are uniformly distributed on the surface of the carbon paper and the interior, and with the increase in the amount of CNFs added, the flocculation

phenomenon increases. The CNFs were evenly distributed on the surface and inside of the carbon paper, and with the increase of CNFs addition, the flocculation situation was aggravated, and the uneven distribution of CNFs will affect the subsequent test results of the carbon paper.
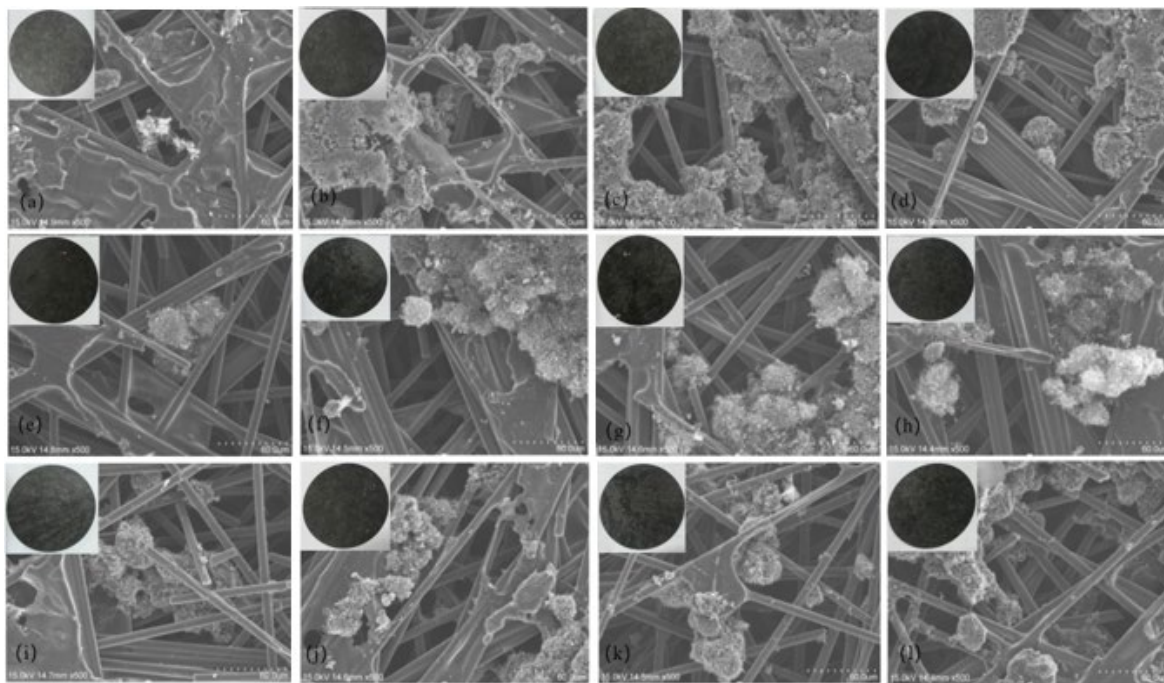
Fig. 13. Carbon paper prepared at 150°C and 3.0 MPa hot pressing condition (a) S-I-5% (b) S-I-10% (c) S-I-15% (d) S-I-20% (e) I-S-5% (f) I-S-10% (g) I-S-15% (h) I-S-20% (i) S&I-5% (j) S&I-10% (k) S&I-15% (l) S&I-20% Physical image and microscopic morphology.

Fig. 13 showed the physical and microscopic morphology of the carbon paper obtained after the S-I, I-S, and S&I preparation processes at 150°C, 3.0 MPa, and hot pressing for 20 min. From the figure, it could be seen that the carbon paper of the three preparation processes had high flexibility, could be bent to a certain extent, and is not easy to break and shatter. The surface of carbon paper was smooth and the fiber interlacing is clearly visible. There were CNFs attached to the surface of carbon paper of the three preparation processes, and the attachment amount of CNFs increased with the increase of the addition amount. The micro-morphology of the carbon paper was observed by SEM image, the carbon fibers were interlaced, and the hot-melted PVA fibers were bonded to the carbon fibers, which had CNFs adhered in clusters. The S-I carbon paper has a large number of CNFs attached between the fibers, and the CNFs are distributed in clusters, as shown in Fig. 13 (a-d). Under the joint action of CNFs and hot-melted PVA fibers, the internal fibers of carbon paper could be closely connected, and the void between fibers was reduced, but there was a flocculation phenomenon, and it was serious with the increase of the addition of CNFs, and the redundancy of CNFs in too many clusters will affect the performance of carbon paper. From Fig. 13 (e-h), it could be found that more CNFs are retained on the surface of I-S carbon paper, and less CNFs enter into the interior of the carbon paper, resulting in insufficient effective connection between the internal fibers and larger inter-fiber gaps. The flocculation phenomenon on the surface

of carbon paper increases with the increase of CNFs addition. From Fig. 13 (i-l), it could be found that S&I carbon paper also has a certain flocculation situation. Through the microscopic morphology, it could be found that CNFs with the phenolic resin immersed into the carbon paper, CNFs with the attachment of carbon fibers and PVA fibers on top of the carbon fibers, and with the hot compression molding in the inter-fiber bridging. Because of the simultaneous spray coating and phenolic resin impregnation, there will be a certain loss of CNFs, so the inter-fiber gap will be a little larger.

3.3.2. Air permeability

Fig. 14 showed the results of gas permeability testing regarding the carbon paper prepared under three process conditions. From the figure, it could be seen that the air permeability performance of carbon paper decreases with the increase of CNFs addition. The group with higher hot pressing temperature and higher pressure has worse air permeability, which was attributed to the fact that the higher temperature and pressure make the carbon paper more compact with smaller inter-fiber pores. From Fig. 14 (c and f), it could be found that under various hot pressing conditions, the air permeability of carbon paper treated by S&I is the best. The reason was that during the simultaneous treatment process of filling CNFs and impregnation of carbon paper, CNFs are retained in the impregnating solution, which does not reach 100% retention, so the carbon paper fiber connection is insufficient, and the internal pores are large, which results in high air permeability. Fig. 14 (a and d) showed the air permeability curve of S-I carbon paper. The poor air permeability of the carbon paper obtained by this preparation method was due to the fact that the vast majority of CNFs were retained between the internal fibers of the carbon paper, which effectively fills up the inter-fiber voids, resulting in a decrease in air permeability. From Fig. 14(b and f), it could be seen that the I-S carbon paper has dense adherent CNFs on the surface, and the air permeability is poor.
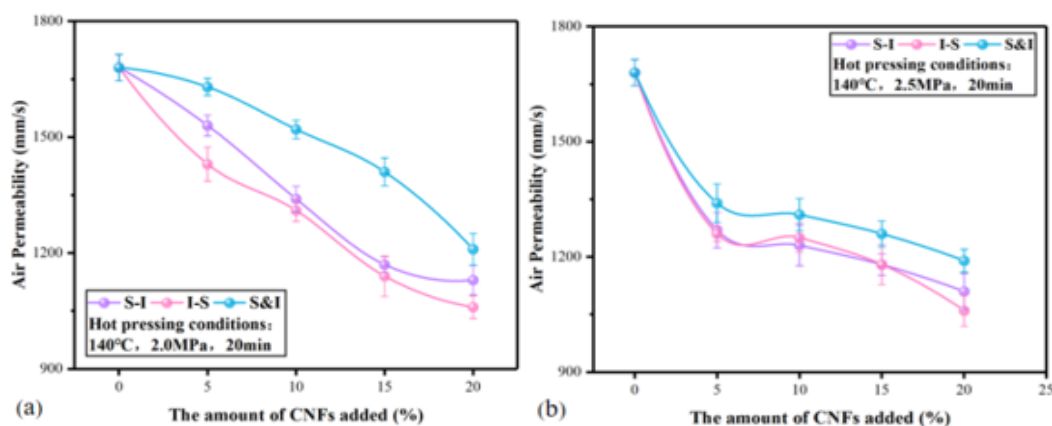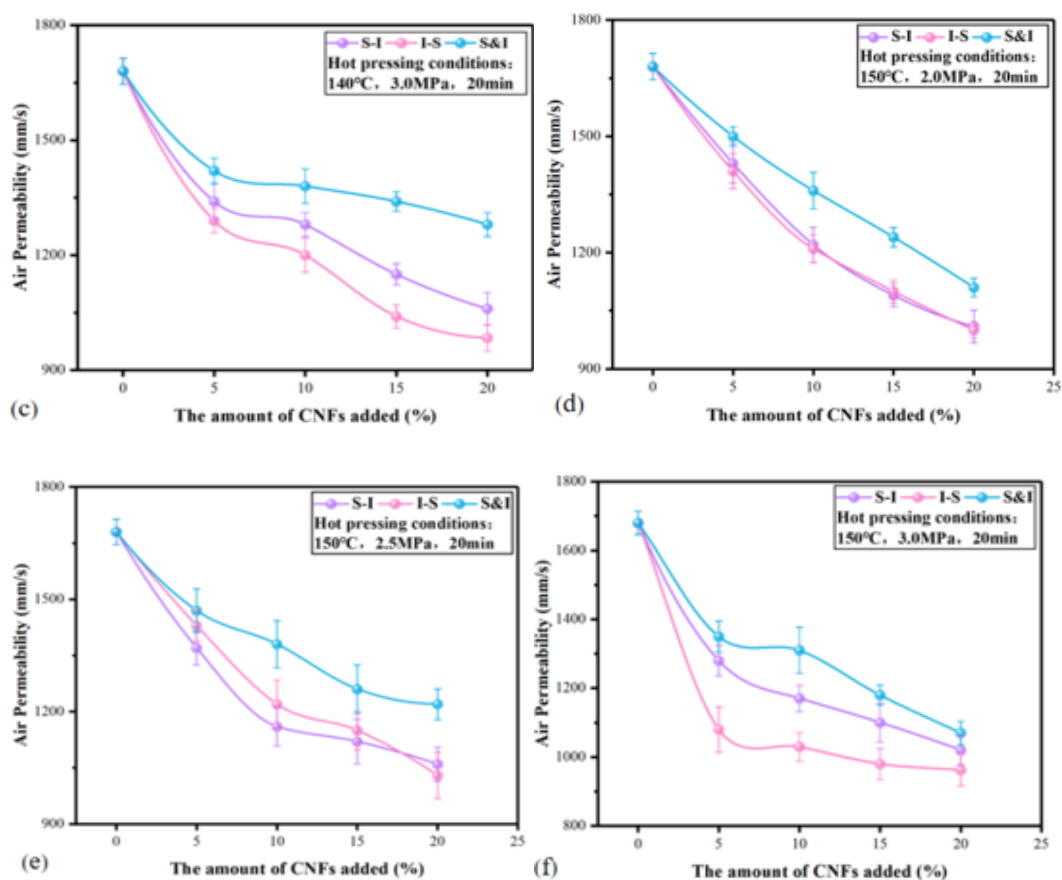
Fig. 14. Effect of different preparation conditions (a) 140℃, 2.0 MPa (b) 140℃, 2.5 MPa (c) 140℃, 3.0 MPa (d) 150℃, 2.0 MPa (e) 150℃, 2.5 MPa (f) 150℃, 3.0 MPa on the permeability of carbon paper.

3.3.3. Electrical resistivity

Fig. 15 showed the results of the conductivity test regarding the carbon paper prepared under three process conditions. As could be seen from the figure, 10% CNFs carbon paper had the lowest resistivity and the best conductivity. Carbon paper under different pressures at 140℃ showed the same trend, with S-I carbon paper having the lowest resistivity and most of the CNFs penetrating inside the carbon paper through impregnation. The hot-melted PVA fibers were connected to the carbon fibers, and the CNFs were attached to the carbon fibers to form a large number of conductive pathways, which improved the electrical conductivity of the carbon paper. As a result, the S-I carbon paper has the lowest resistivity when filled with different amounts of CNFs. I-S carbon paper had a high resistivity due to the large surface area covered with CNFs, which had fewer effective conductive paths. Due to the simultaneous spraying and impregnation processes, the S&I carbon paper loses a portion of its CNFs, resulting in a lower content of CNFs on the carbon paper, a serious lack of conductive paths between carbon fibers, the highest resistivity, and the worst electrical conductivity compared to the other two processes with the same amount of filling. Looking at the curves of the six hot pressing conditions together, it could be concluded that the carbon paper had the lowest resistivity at 150℃ and 3.0 MPa. Higher temperatures as well as pressures will make the carbon paper tighter, with smaller inter-fiber gaps, more effective conductive pathways between

fibers, and a decrease in its resistivity. When CNFs are added at 10%, CNFs do not cause large-scale flocculation, and the connection between carbon fibers was more effective. Therefore, in the curve, often the resistivity of the group with 10% addition amount was a little lower. From this, it could be deduced that when the filling amount of CNFs was controlled at about 10%, the resistivity of S-I carbon paper was the lowest and its electrical conductivity is the best when the hot pressing condition is 150°C and 3.0 MPa.
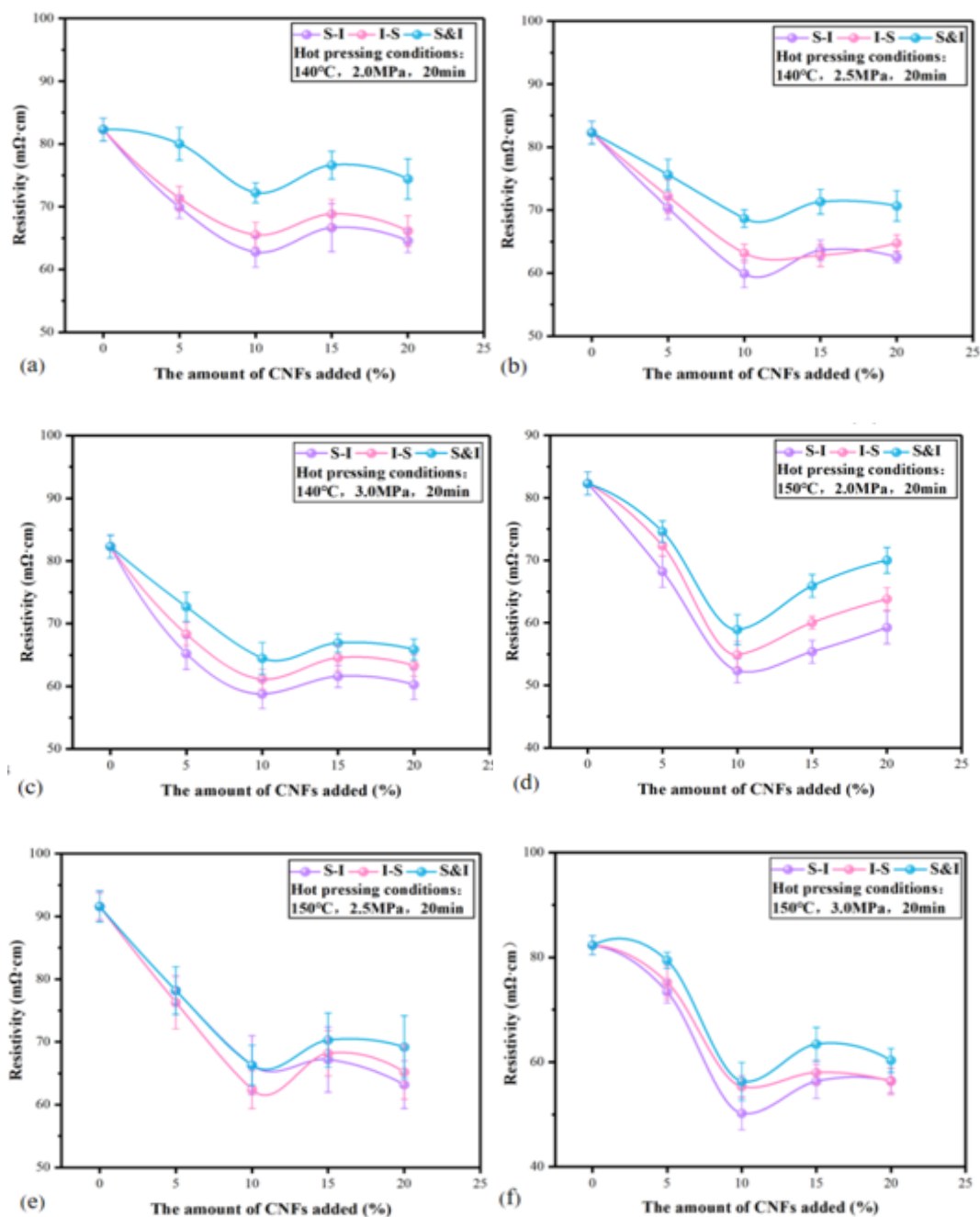
Fig. 15. Effect of different preparation conditions (a) 140°C, 2.0 MPa (b) 140°C, 2.5 MPa (c) 140°C, 3.0 MPa (d) 150°C, 2.0 MPa (e) 150°C, 2.5 MPa (f) 150°C, 3.0 MPa on the permeability of carbon paper.

3.3.4. Physical property

Fig. 16 showed the stress test results regarding the carbon paper prepared under three process conditions. From the figure, it could be seen that 10% CNFs is the optimal addition under various hot-pressing conditions and different carbon paper processing conditions, and its corresponding stresses are all optimal. From Fig. 16 (a and d), it could be seen that the stress data of S-I carbon paper is optimal, which is related to the fact that CNFs are concentrated in the interior of the carbon paper with smaller inter-fiber gaps, and the CNFs and the hot-melted PVA fibers work together to make the internal fiber structure of the carbon paper compact, which greatly improves the physical properties of the carbon paper. From Fig. 16 (b and e), it could be found that the stress of I-S carbon paper under each filling amount was not much different from that of carbon paper of S-I group, which was much higher than that of the control group. The reason was that the presence of a large number of CNFs between the fibers or on the surface of the carbon paper can effectively enhance the physical properties of the carbon paper, and the stress increases significantly. Compared with the other two processes, Fig. 16(c and f) showed that the weaker improvement of the physical properties of S&I carbon paper is inextricably linked to the fact that its CNFs are not 100% coated.
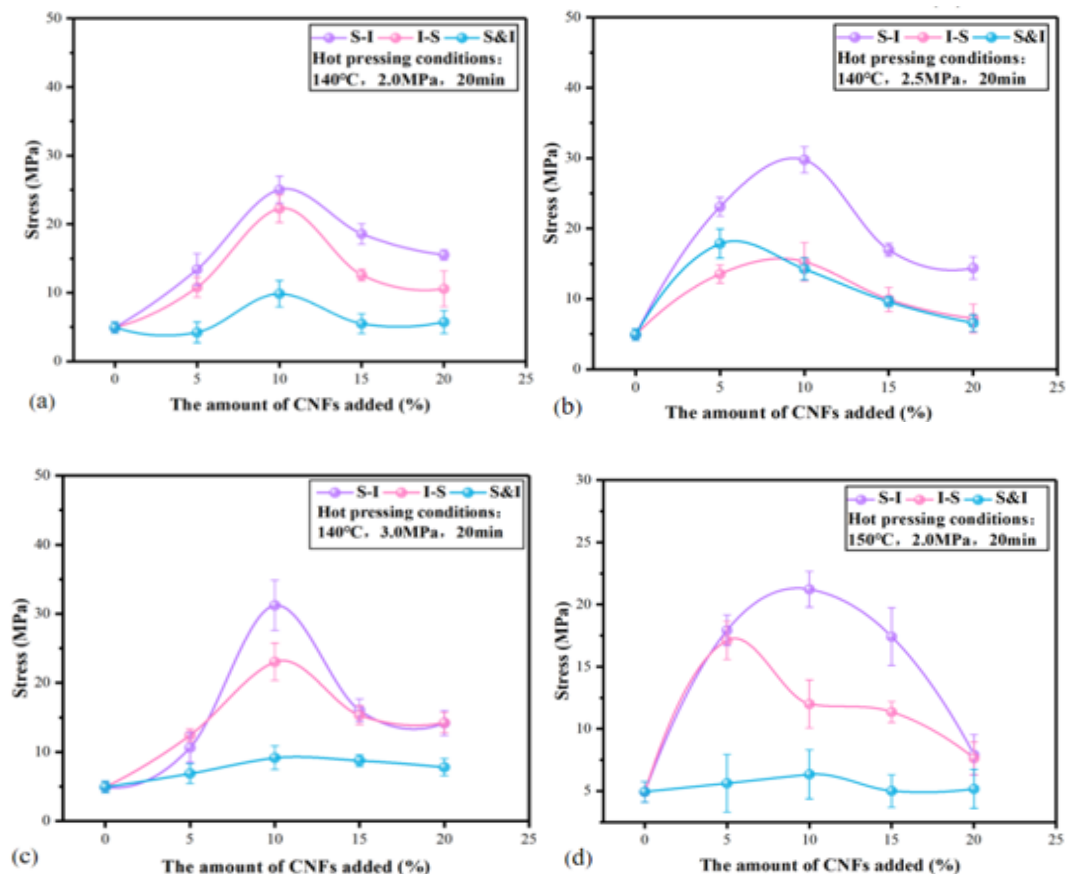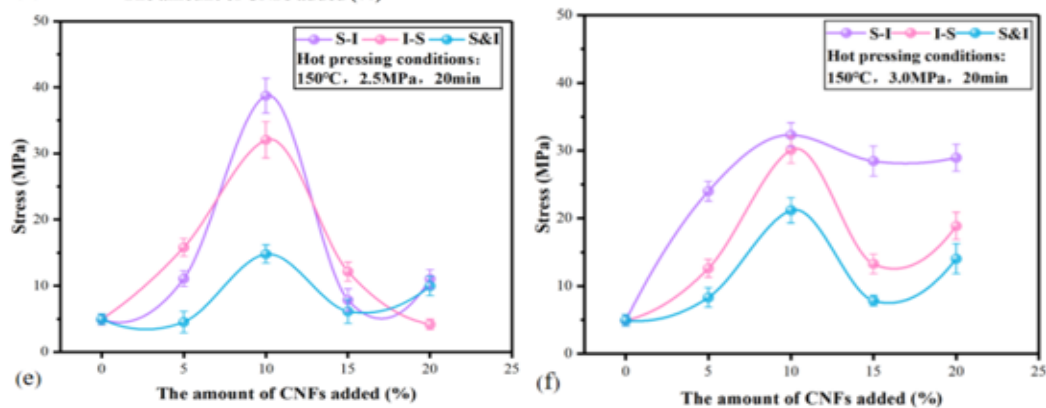
Fig. 16. Effect of different preparation conditions (a) 140℃, 2.0 MPa (b) 140℃, 2.5 MPa (c) 140℃, 3.0 MPa (d) 150℃, 2.0 MPa (e) 150℃, 2.5 MPa (f) 150℃, 3.0 MPa on the stress of carbon paper.

3.3.5. Tensile strength

Fig. 17 showed the tensile strength of carbon paper prepared by S-I, I-S and S&I processes after hot pressing at 150℃ and 2.0-3.0 MPa. As can be seen from the figure, the tensile strength of carbon paper filled with 10% CNFs is optimal. The addition of appropriate mass proportion of CNFs not only effectively avoids the negative effects of CNFs aggregation, but also plays a bridging role in connecting the carbon fibers, resulting in a better bonding between the carbon fibers and a higher tensile strength than that of the carbon paper with other additions. From Fig. 17 (a-c), it could be found that the addition of CNFs enhances the tensile strength of S-I carbon paper, which was significantly higher than that of the blank group without CNFs, and reaches the optimum at 10% CNFs addition. The reason was that the hot-melt PVA fibers cover a large area on the carbon fibers, and the sprayed CNFs are attached to them, and the pore size changes are small, which improves the tensile strength of the carbon paper. Fig. 17 (d-f) showed the tensile strength curves of I-S carbon paper, and the tensile strength is optimal when the addition amount of CNFs is 10%. In addition, the tensile strength of carbon paper with other CNFs additions was not high, which was due to the fact that the post-sprayed CNFs only remain on the surface, and the performance of the carbon paper only improves on the surface. The carbon paper with excessive CNFs addition also produces serious agglomeration after hot pressing, and a small portion of CNFs enters into the interior, which negatively affects the improvement of the tensile strength of the carbon paper. However, it was shown from Fig. 17 (g-i) that the tensile strength of carbon paper with S&I preparation conditions was hardly improved compared with the blank group without CNFs. Simultaneous spraying and impregnation affect the spraying effect of CNFs. A part of the spray-coated CNFs remained in the impregnation solution, resulting in less attached CNFs, insufficient effective area between fibers inside the carbon paper, and large inter-fiber voids, which affected the tensile strength.

(a)

(b)

(c)

(d)

(e)

(f)

(g)

(h)

(i)
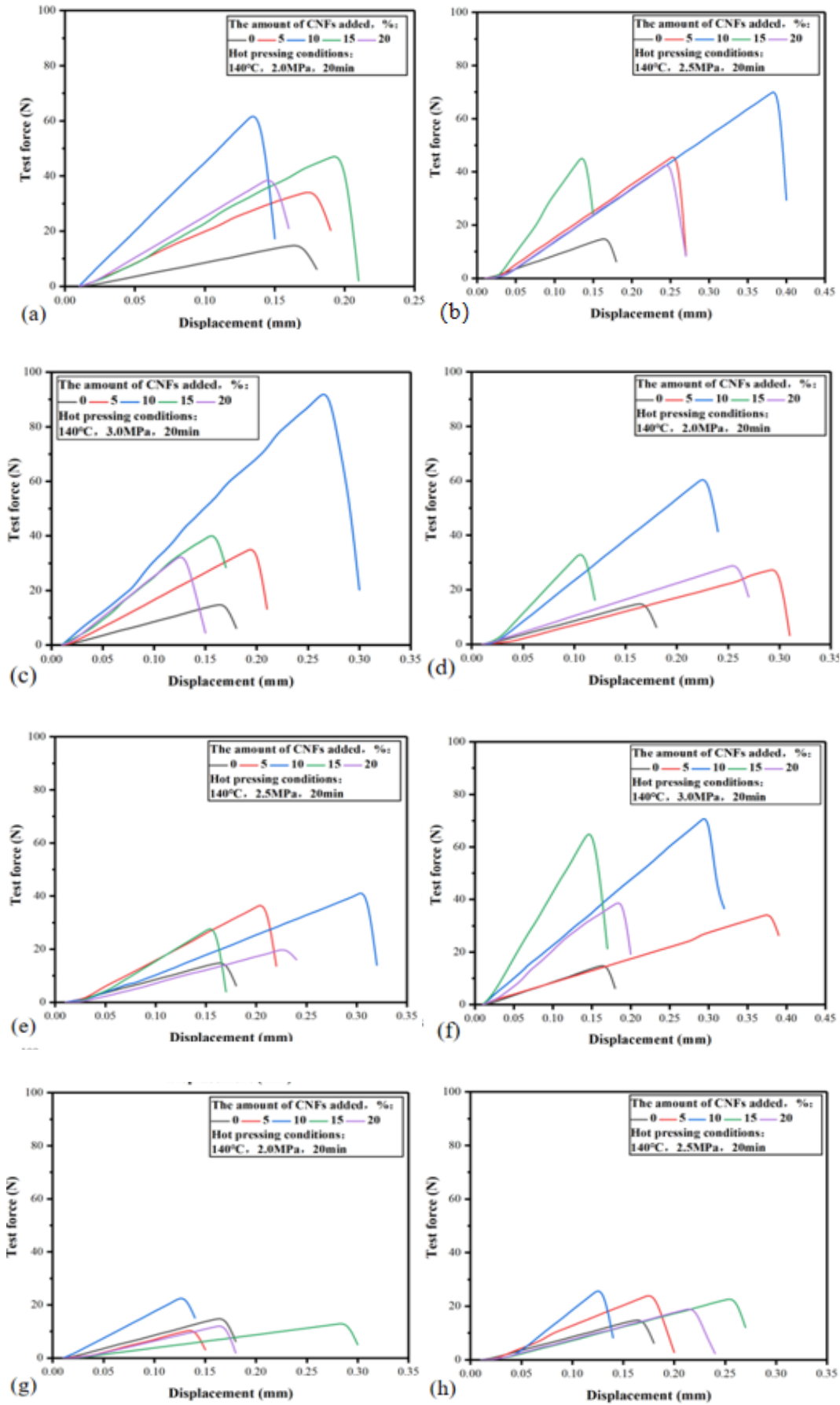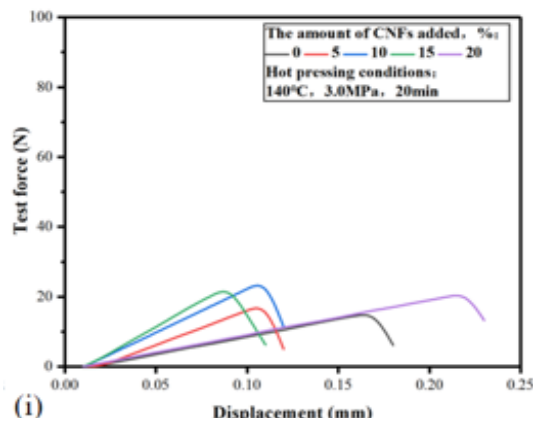
Fig. 17. Effect of carbon paper of S&I on tensile strength under different preparation conditions (a) (b) (c) S-I (d) (e) (f) I-S (g) (h) (i)S&I.

(a)

(b)

(c)

(d)
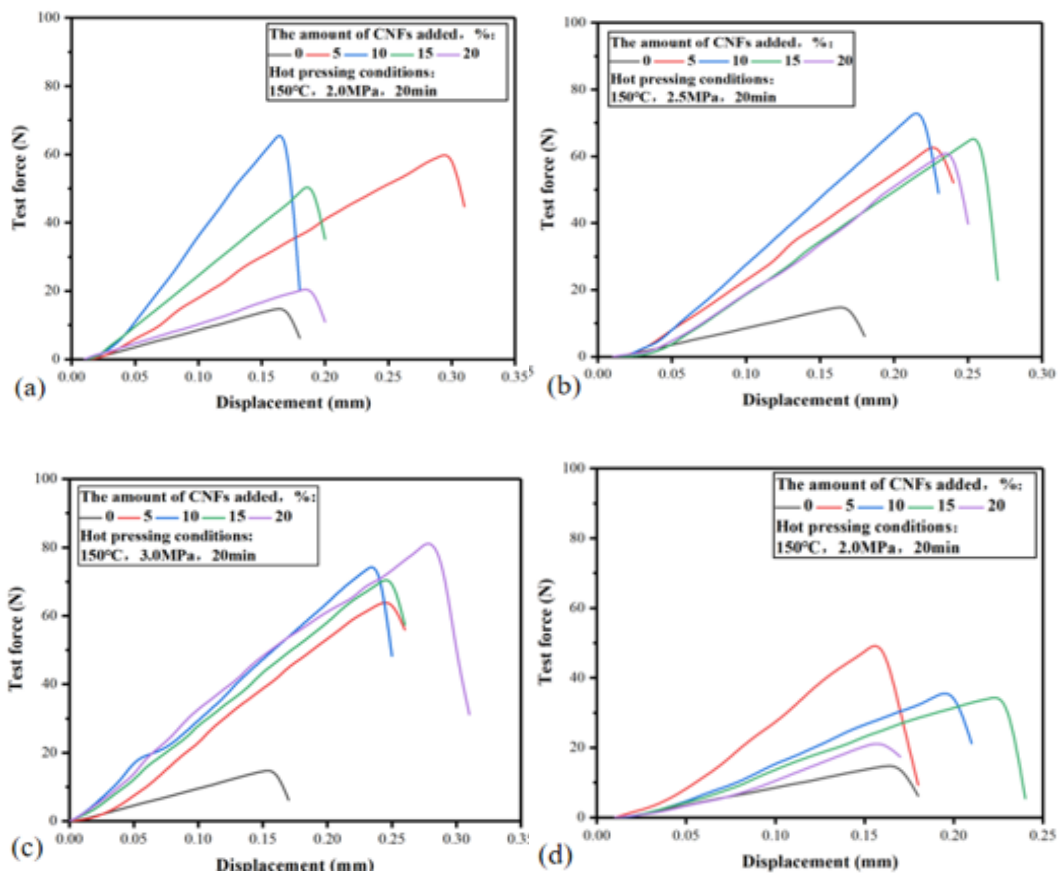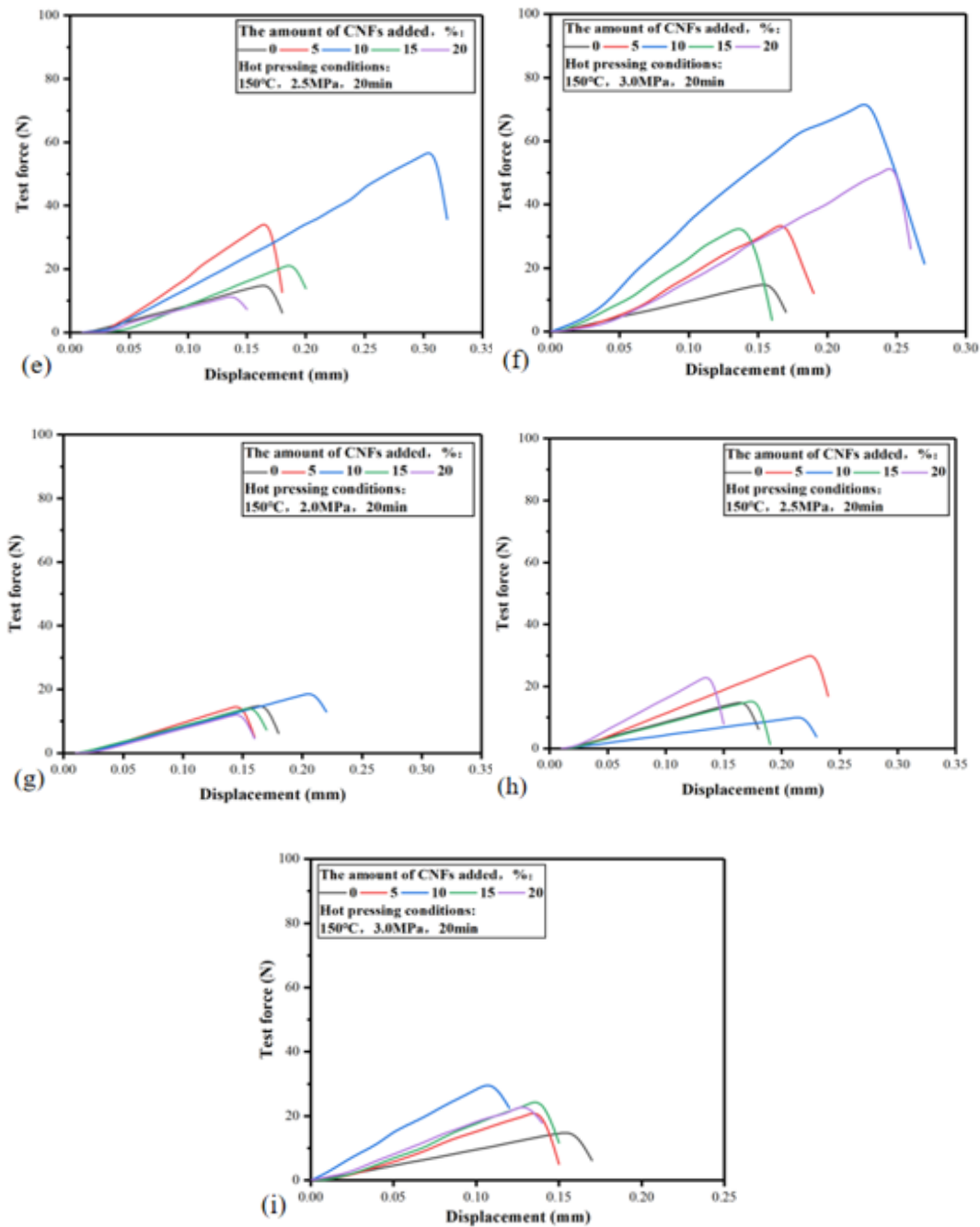
Fig. 18. Effect of S&I on tensile strength of carbon paper at different preparation conditions (a) (b) (c) S-I (d) (e) (f) I-S (g) (h) (i) S&I.

Fig. 18 showed the tensile strength of carbon paper prepared by S-I, I-S and S&I processes after hot pressing at 150°C and 2.0-3.0 MPa. Based on the curves in the figure, it could be concluded that the tensile strength of carbon paper with an addition of 10% CNFs was optimal. The addition of appropriate amount of CNFs will have an effect on the improvement of the physical properties of carbon paper. From Fig. 18 (a-c), it could be found that the amount of added CNFs had a significant effect on the S-I carbon paper. Compared with the blank control without added CNFs, the addition

of CNFs can effectively improve the tensile strength of carbon paper, and the tensile strength of S-I-10% carbon paper is optimal. Hot pressing after impregnation can bring the sprayed CNFs uniformly onto the hot-melted PVA fibers inside the carbon paper, forming a tightly built-up bridge structure with dense inter-fiber connections and smaller voids. From Fig. 18 (d-f), it could be found that the tensile strength of I-S-10% carbon paper is optimal, while the data are significantly lower than that of S-I carbon paper when the additive amount was 5%, 10% and 20%. The reason may be that after the I-S treatment, the CNFs only stay on the surface of the carbon paper, and the excessive redundancy of CNFs also causes the surface flocculation phenomenon, and the lack of internal CNFs lead to large internal voids and few effective connections in the carbon paper. From Fig. 18 (g-i), it could be seen that the carbon paper treated with S&I showed a slight increase in tensile strength compared with the blank control group, but the effect was not significant. Spraying and impregnation were carried out at the same time, and the presence of residual CNFs in the impregnation solution, which failed to achieve 100% spraying effect, led to insufficient connection between carbon fibers of carbon paper, thus affecting the tensile strength of carbon paper under this treatment condition.

4. Conclusion

A strategy to obtain high-performance carbon paper by doping with carbon nanofibers was proposed. Specifically, at a carbon nanofiber filling level of 10%, the electrical conductivity and mechanical properties of the carbon paper were significantly improved, which was essential for optimizing the performance of PEMFCs. The optimal process flow identified was the impregnation followed by the S-I method, which contributed to a more homogeneous distribution of carbon nanofibers, resulting in improved electrical and mechanical properties. This process was combined with a 10% addition of carbon nanofibers under hot pressing conditions at 150°C and 3.0 MPa, which contributed to the densification and performance enhancement of the carbon paper. A strategic approach was provided for the fabrication of carbon paper capable of improving the efficiency and durability of proton exchange membrane fuel cells.

Acknowledgement

References

[1] K. He, C. Zhang, Q. He, Q. Wu, L. Jackson, L. Mao, International Journal of Hydrogen Energy 45(56) (2020) 32355-32366; https://doi.org/10.1016/j.ijhydene.2020.08.149

[2] Y. Akimoto, K. Okajima, Y. Uchiyama, Energy Procedia 75 (2015) 2015-2020; https://doi.org/10.1016/j.egypro.2015.07.261

[3] A. Benmouna, M. Becherif, D. Depernet, F. Gustin, H.S. Ramadan, S. Fukuhara, International Journal of Hydrogen Energy 42(2) (2017) 1534-1543; https://doi.org/10.1016/j.ijhydene.2016.07.181

[4] P. Singh, A. Sandhu, International Journal of Energy Research 46(13) (2022) 18212-18224; https://doi.org/10.1002/er.8437

[5] S.C. Tan, J.J. Li, L.J. Zhou, P. Chen, J.T. Shi, Z.Y. Xu, Polymers 10(10) (2018); https://doi.org/10.3390/polym10101072

[6] D.H. Tian, Z.C. Han, M.Y. Wang, S.Q. Jiao, International Journal of Minerals Metallurgy and Materials 27(12) (2020) 1687-1694; https://doi.org/10.1007/s12613-020-2026-z

[7] W.J. Zhang, Y.L. Wang, Ceramics International 49(6) (2023) 9371-9381; https://doi.org/10.1016/j.ceramint.2022.11.104

[8] X.W. Fu, J. Wei, F.D. Ning, C. Bai, Q.L. Wen, H.Q. Jin, Y.L. Li, S.Y. Zou, S.F. Pan, J.F. Chen, S.W. Deng, X.C. Zhou, Journal of Power Sources 520 (2022); https://doi.org/10.1016/j.jpowsour.2021.230832

[9] A. Pokprasert, S. Chirachanchai, Polymer 265 (2023); https://doi.org/10.1016/j.polymer.2022.125583

[10] Y. Garsany, R.W. Atkinson, B.D. Gould, R. Martin, L. Dubau, M. Chatenet, K.E. Swider-Lyons, Journal of Power Sources 514 (2021); https://doi.org/10.1016/j.jpowsour.2021.230574

[11] Z.Y. Wu, S.Y. Qin, Y.M. Liu, J. Hu, X. Li, B.W. Zhang, C.H. Zhang, K. Zhang, J.X. Sun, H. Pan, X. Liu, Journal of Industrial Textiles 53 (2023); https://doi.org/10.1177/15280837221149214

[12] J. Sim, M. Kang, K. Min, E. Lee, J.Y. Jyoung, Journal of Mechanical Science and Technology 36(9) (2022) 4825-4838; https://doi.org/10.1007/s12206-022-0841-z

[13] J.X. Liu, H. Guo, F. Ye, C.F. Ma, Energy 119 (2017) 299-308; https://doi.org/10.1016/j.energy.2016.12.075

[14] J. Molina, A. Valero-Gómez, F. Bosch, International Journal of Hydrogen Energy 47(97) (2022) 41223-41235; https://doi.org/10.1016/j.ijhydene.2022.03.151

[15] W. Yang, J. Wang, S. Gao, H. Zhang, H. Wang, Q. Li, Journal of Advanced Ceramics 11(11) (2022) 1735-1750; https://doi.org/10.1007/s40145-022-0644-9

[16] D. Jiang, H. Chen, H. Xie, K. Cheng, L. Li, K. Xie, Y. Wang, Environmental Research 221 (2023) 115308; https://doi.org/10.1016/j.envres.2023.115308

[17] J. Park, L.K. Kwac, H.G. Kim, H.K. Shin, Molecules 27(6) (2022) 1842; https://doi.org/10.3390/molecules27061842

[18] C. Song, M. Liu, L. Du, J. Chen, L. Meng, H. Li, J. Hu, Journal of Power Sources 548 (2022) 232012; https://doi.org/10.1016/j.jpowsour.2022.232012

[19] N. Liu, L.L. Jiang, Journal of Intelligent Material Systems and Structures 31(14) (2020) 1716-1730; https://doi.org/10.1177/1045389X20932216

[20] E. Ismar, A.S. Sarac, Polymer Bulletin 75(2) (2018) 485-499; https://doi.org/10.1007/s00289-017-2043-x

[21] M. Yu, B.J. Xin, Z.M. Chen, Y. Liu, Fibers and Polymers (2023); https://doi.org/10.1007/s12221-023-00387-2

[22] Z.F. Zhao, J.H. Gou, A. Khan, Journal of Nanomaterials 2009 (2009);
https://doi.org/10.1155/2009/325769